Centre for Radio Science
The University of Western Ontario
London, CANADA.

Experimental Determination of the Structure of Multipath Propagation on Terrestrial Microwave Links.

T. S. Merritt, A. R. Webster and H. Wong.

Final Report.
D.S.S. Contract #
36001-6-3532/01-ST

December, 1987.

2°

Experimental Determination of the Structure of Multipath Propagation on Terrestrial Microwave Links.

A Final Report

under

Department of Supply and Services

Contract # 36001-6-3532/01-ST

Submitted to

Communications Research Centre,

Department of Communications,

Ottawa, Canada.

by

Centre for Radio Science,

The University of Western Ontario,

London, Canada.

Principal Investigator: A. R. Webster.

Research Associates: T. S. Merritt, H. Wong.

Scientific Authority at CRC
Dr B. Segal.

December, 1987.

TABLE OF CONTENTS.

I. INTRODUCTION

One of the fundamental problems facing the radio engineer is the occurrence of multiple propagation paths (rays) between the terminals of a microwave link. These undesirable rays may be the result of reflections from the earth's surface or disturbances in the normal refractive gradient of the lower atmosphere (atmospheric multipath). Severe fading may occur when two or more rays of comparable amplitude arrive within the beam width of the receiving antenna. Multipath is especially harmful to wide band digital radio systems due to its frequency selective nature [1].

Efforts to devise systems that are less susceptible to atmospheric effects have been hampered by a lack of experimental data on the distribution of multipath propagation parameters. The data available in the literature has, until recently, been limited to specific observations of angles-of-arrival, amplitudes, and delay times of the individual multipath components [for example, 2-6].

This report deals with the distribution of multipath parameters obtained from data collected during the late summer and fall of 1986 on a 30 km (Uniondale-London) link in Southwestern Ontario. A uniformly spaced vertical antenna array developed under a previous contract (D.S.S. 24ST.36001-5-3549) was used to sample the amplitude and relative phase of the received signal through a vertical aperture. The number of resolved

propagation paths, angles-of-arrival, and amplitudes were obtained from these data using the Fast Fourier Transform (FFT). This project is a continuation of the work started by Webster and Scott [6] using an antenna array which has been improved in resolution, range, portability, and reliability.

The operation of this system was resumed in 1987 on the same link starting in May and continuing until early August. At that time, the whole system was transferred to the 41 km London-Russelldale link operated by Bell Canada and data recorded until the end of October, 1987. All of these 1987 data are stored on magnetic tape for further processing.

In addition to the operation of the microwave system, a vertical acoustic sounder has been operated at the Centre for Radio Science starting in the late Fall 1986 and continuing in 1987 from June to November. Much of the activity here has been in the development of hardware and software to digitize and store the raw data on magnetic tape; a limited amount of processing has been carried out at the time of writing.

II. ANGLE-OF-ARRIVAL MEASUREMENTS.

II.1 The Experimental Method.

Under multipath conditions, the received signal may be modelled as the sum of a small number of plane waves. For N propagation paths, the received signal "r" at a height "x" above an arbitrary reference point is given by,

$$r(x) = \sum_{i=1}^{N} A_i \cdot \exp[j\{\frac{2\pi x}{\lambda}.\sin\theta_i - \delta_i\}] \quad (1)$$

where λ is the wavelength, "A_i" the ray amplitudes, "θ_i" the ray angles-of-arrival, and "δ_i" the phase delays at x = 0. The angle-of-arrival spectrum "$R(\xi)$" is given by the Fourier transform of the received signal over a vertical aperture,

$$R(\xi) = \int_{-L/2}^{L/2} r(x).\exp(-j2\pi\xi x).dx$$

$$= \sum_{i=1}^{N} A_i.L.Sa\left[\pi\frac{L}{\lambda}(\theta_i - \xi\lambda)\right].e^{-j\delta_i} \quad (2)$$

where "L" is the length of the aperture, "ξ" is the transform variable, Sa(u) is the sampling function sin(u)/u and the approximation $\sin\theta \approx \theta$ has been applied. Several properties of (2) are of interest: (i) each term in the summation corresponds to one of the individual rays, (ii) the amplitude of each term is proportional to the amplitude of the corresponding ray, (iii) each term is shifted along the "ξ" axis by an amount proportional to the angle-of-arrival (θ_i) of

the corresponding ray, and (iv) the width of the sampling function peak is inversely proportional to the aperture length in wavelengths.

If the individual rays are separated sufficiently in angle-of-arrival so that the individual sampling function peaks do not significantly interfere with each other, then the number of propagation paths, their amplitudes, and their angles-of-arrival can be determined from the positions and amplitudes of the peaks in the angle-of-arrival spectrum. Sidelobe interference can be reduced by using an appropriate weighting function, at the expense of a wider main peak.

It will be noted that the above discussion is also true for a discretely sampled aperture, using the discrete Fourier transform to obtain the angle-of-arrival spectrum.

The minimum resolution, or the minimum angle-of-arrival separation for which two rays will be resolved as separate peaks in the spectrum, is dependent mainly on the length of the aperture and the weighting function used; some influence on the resolution is exerted by the delay between adjacent rays. The resolution for the 40 dB Dolph Chebyshev weighting used here is about 0.10 - 0.14^{o} depending on the delay involved; Fig II-14(a) shows the response of the data analysis routine used to determine the angular separation between adjacent rays obtained

by synthesizing data in difference increments of 0.0125^{o} in AOA, 10^{o} in delay phase and 0.1 (1.0 down to 0.1) in amplitude.

The maximum unambiguous range "θ_{max}", that is the maximum range in angle-of-arrival that can be measured without aliasing, is given by:

$$\theta_{max} = \pm \frac{1}{2} \cdot \arcsin\left(\frac{\lambda}{d}\right) \qquad (3)$$

where "d" is the sampling interval, or spacing between the array elements. For the measurements presented here, λ= 0.0108m and d = 0.75m giving $\theta_{max} = \pm 0.70°$.

II.2 The Experimental Apparatus

The antenna array consists of sixteen uniformly spaced pyramidal horns mounted vertically with a separation of 0.75 m. A 0.6 m diameter parabolic dish antenna is mounted near the centre of the array to provide a reference signal for phase measurements and receiver phase locking. A single 16.530 GHz local oscillator and the waveguide arrangement shown in Fig. II-1 are used to convert the 16.650 GHz received signals to the first intermediate frequency (IF) of 120 MHz. The waveguide arrangement was designed so that it could be pressurized with nitrogen to exclude water vapour. A compromise was made so that the array could be easily assembled at the receiving site, resulting in unequal path lengths from the local oscillator to each mixer. The expansion or contraction of the waveguide with

ambient temperature changes will result in small errors in the phase measurements. This effect is predictable (1° of phase per °C temperature change per 100 wavelengths of WR-62 waveguide), and was corrected using temperature data from the London Airport Meteorological Station [7].

A four bit control signal and the switching arrangement shown in Fig. II-2 are used to select one of the sixteen array element signals. The selected signal and the reference channel signal are connected to the receiver through two 75 m lengths of RG8/U coaxial cable. The four control signals are sent to the switches using RS232C signal levels and a similar length of shielded multiconductor cable. Power for the local oscillator, switches, and amplifiers is provided through an RG58/U cable, also 75 m long. A 102 MHz local oscillator reference signal is returned on the power cable for diagnostic purposes.

The receiver, shown in Fig. II-3, contains two similar channels that use three stages to provide the intermediate frequencies of 53.17 MHz, 10.70 MHz, and 82.95 KHz. The Automatic Gain Control (AGC) circuiting detects the amplitude of the received signals at the 10.70 MHz IF and controls the gain of the 53.17 MHz and first 10.70 MHz amplifiers to provide a dynamic range of 60 dB. The AGC voltages are also amplified and shifted to the correct levels for the microcomputer's analogue to digital (A/D) converter. The two 82.95 KHz signals and the 21.2 MHz

clock signal are used to determine the phase of the array channel signal with respect to the reference signal. The eight bit phase value is determined by counting the number of clock pulses between the falling edges of the two 82.95 KHz signals.

An important feature of the receiver is the phase locking and local oscillator arrangements. The reference channel signal is phase locked to the receiver's master oscillator, providing phase coherence throughout the receiver and ensuring that the received signals remain within the receiver's narrow bandwidths (30 KHz for the reference channel and 13 KHz for the array signal channel).

The system timing, data collection, and data storage are controlled by a Zenith personal computer. At the beginning of every second the computer samples the reference channel amplitude, the amplitude of each array signal, and the phase of each array signal relative to the reference signal. The reference signal amplitude is always available from the AGC voltage of the receiver's reference channel, and is obtained through one channel of a multi-channel A/D converter. Since only one receiver channel is provided for the sixteen array signals, the computer must select the signal to be measured using the switching arrangement described earlier. A 3ms delay, inserted after selecting a signal, allows the receiver AGC voltage to settle. The array signal amplitudes are

obtained through a second channel of the multi-channel A/D converter. Sixteen separate phase measurements are made for each signal. These phase values are checked for jitter around 0 and 360° and averaged. The data collection cycle for the entire array takes approximately 50 mS, and produces one twelve-bit reference amplitude, sixteen eight-bit array signal amplitudes, and sixteen eight-bit phase values. The data is stored with the date, time, and other information as a 2K byte record on magnetic tape, representing one minute of data.

II.3 The Data Analysis and Results

The antenna array was installed at the Centre for Radio Science in London, Ontario to receive a 16.650 GHz continuous wave (CW) signal transmitted from an Ontario Hydro tower near Uniondale, 30 km northeast of London. Details of the path are given in Table 1. The path profile, using the flattened earth representation, is shown in Fig. II-4 with the propagation path and first Fresnel radius for a refractivity gradient of -39 NU/km. Data were collected for this path during the late summer and fall of 1986. During this time, ten nights of severe multipath fading were observed. The results presented in this paper are based on 123.5 hours of fast fading (multipath) data representing 444,600 sweeps of the array. The data were selected using meteorological information from the London Airport, indicating calm conditions and the absence of precipitation.

The cumulative distribution of the reference channels received signal level is shown in Fig. II-5, where 0 dB represents the normally received signal level. The slope of distribution is very near the 10 dB per decade expected for multipath fading, indicating that this data is representative of typical multipath fading periods.

Examples of the angle-of-arrival spectra obtained during a) undisturbed propagation conditions and b) multipath conditions are presented in Fig. II-6. The angle-of-arrival spectra were obtained by i) subtracting the resting levels of amplitude and phase from the array signals; ii) correcting the phase values for ambient temperature changes; iii) weighting the amplitudes with a 40 dB Dolph-Chebyshev window; iv) padding the data with zeros; and v) performing a 64 point Fast Fourier Transform (FFT). The resting levels were determined by averaging the amplitudes and phases of the array signals for several one hour periods of undisturbed propagation distributed throughout the data. **As a result, all angles-of-arrival measured during this experiment are with respect to the angle-of-arrival of the signal for undisturbed propagation conditions.**

Fig. II-7 shows the angle-of-arrival spectrum as a function of time for a three minute period. A mirror image of the plot is included to reveal features that would otherwise be hidden behind the peaks. The reference channel amplitude for the same

time period is shown in Fig. II-8, revealing two fades at the points marked A and B. The corresponding times in Fig. II-7 illustrate that these fades are due to the interaction of at least three large amplitude rays and other lower amplitude rays.

The time variation of the individual ray angles-of-arrival and amplitudes are further illustrated in Fig. II-9. The angles-of-arrival are shown in Fig. II-9(b) with trace widths proportional to the ray amplitudes in dB. The corresponding ray amplitudes are given in Fig. II-9(c). Both plots were generated by fitting a parabola through the three points closest each peak in the angle-of-arrival spectrum and calculating the position and amplitude of the peaks. A threshold, 20 dB below the strongest peak in each spectrum, was used and no peaks below it were included. The reference channel amplitude is also included as Fig. II-9(a) for comparison.

Several interesting observations can be made from Figs. II-9(b) and 9(c); i) the angle-of-arrival of the strongest path is consistently elevated by approximately 0.15°; ii) the reference channel amplitude follows closely the amplitude of the strongest ray, except when deep, sharp fades occur; iii) the deep fades occur where the multiple rays appear to be either converging (1:15 EDT) or diverging (1:23); and iv) the angle-

of-arrival patterns at 1:15 EDT and 1:23 EDT are very similar, though inverted in time.

While specific examples of multipath events are of interest in determining the causes of multipath fading, statistical distributions of multipath parameters are considered more useful for communications systems design. The distributions at the number of paths, their angles-of-arrival, and amplitudes presented here were obtained using the methods described above. In all cases the 40 dB Dolph-Chebyshev weighting was used, and peaks more than 20 dB below the strongest of each spectrum were not included.

The distribution of the number of resolved propagation paths is given in Fig. II-10. Under multipath conditions (two or more rays), three rays occurred most often. This is consistent with ray tracing results [8] which predict an odd number of propagation paths.

The cumulative distribution of the three strongest ray amplitudes and the reference channel amplitude are presented in Fig. II-11 using probability coordinates. The strongest ray was received above the normal level for a large percentage of time. The second and third amplitude rays were seldom enhanced.

The distributions of angle-of-arrival for the three strongest rays are presented in Figs. II-12 and II-13. The strongest ray was elevated above the normal (zero) angle-of-arrival for the majority of the time. The second and third rays occurred both above and below, with the second ray occurring more often above and the third ray occurring more often below the normal angle-of-arrival. The valleys in the centre of Figs. II-12(b) and (c) are due in part to the minimum resolution of the system, which prevents closely spaced rays from being resolved (see Fig. II-14(a)). The absence of data at the ends of the distributions indicate that the angle-of-arrival range of the system was sufficient to prevent aliasing.

The distribution of the magnitude of the angle-of-arrival separation between the strongest and second rays is given in Fig. II-14. Here, an attempt is made to partially allow for the limited resolution; Fig II-14(b) shows the output from the analysis routine and Fig II-14(c) this same information divided by the response shown in Fig. II-14(a). It appears that the peak in separation in the interval 0.15 - 0.20^{o} is genuine. Fig. II-15 gives the cumulative distribution of angle-of-arrival separations between the strongest and second, and strongest and third rays.

III ACOUSTIC SOUNDER MEASUREMENTS.

As mentioned previously, an acoustic sounder (supplied by the Communications Research Centre) was acquired in the Fall of 1986 and put into operation at that time. Basically an acoustic radar using short pulses of sound at a frequency usually in the order of 1 to 2 kHz, the technique relies on the enhanced reflection from (horizontal) layers over which the temperature changes rapidly. This is one of the requirements for layering which influences microwave propagation and information on the occurrence and distribution with height of such layers, obtained with simultaneous microwave measurements is of some value.

The standard unit uses metallized paper and a high voltage "wiper" to produce a scanned echo strength versus height plot as illustrated in Fig. III-1. This raw information is good from the pictorial point-of-view but presents significant difficulties when automated reduction is attempted. Part of the effort since its arrival has been directed at digitizing the data and storing on 40 MByte cartridge tapes for later processing. The development of appropriate software has been pursued and the reproduction of the "original picture" on a standard printer achieved as a first step (Fig. III-2). The next stage is to scan such records digitally to extract such information as the times of occurrence and the height

distribution of the layers as they occur and relate all of this to the effects on microwave propagation. An example is shown in Fig. III-3 where multiple rays are observed at the time of just such a layer (see Fig. III-2); the sounder was located at the Centre for Radio Science which is about 2 km off the end and in line with the Bell Canada microwave path. In spite of the physical separation, the persistence of the layer suggests widespread coverage so that the speculative relationship between observed layer and resultant multipath would appear to be reasonable.

Further developments being pursued with the sounder include a redesigned transmit/receive section to be inserted inside a portable personal computer; this, it is hoped, will allow the deployment of multiple units in the future.

IV. DISCUSSION

The results presented here are part of an ongoing program aimed at providing information on the occurrence and nature of tropospheric multipath propagation.

The main microwave system was designed to resolve multipath into its separate components and the wide aperture array approach is felt to be effective in this. The recording of the raw complex amplitude across the array allows decisions to be made at a later time on the processing approach to be used. To date, this has been to apply the Fourier transform to appropriately weighted basic data. While there are drawbacks in terms of resolution, there are a number of advantages over other methods:

1. It is robust, being relatively insensitive to small amplitude and phase discrepancies and there is no danger of non-convergence problems as in, for example, curve-fitting methods.
2. It is computationally efficient, allowing the processing of large amounts of data.
3. It is physically significant, being the mathematical equivalent of swinging the beam of a very large antenna.
4. It involves no assumptions about the number of propagation paths.

In the application of the technique, the sampling interval of 1 second appears to be sufficient to capture the variations in the individual paths (Fig. 7) while the range in angle-of-arrival (1.4^{o}), determined by the element spacing, appears to be sufficiently wide to avoid aliasing problems as evidenced by the few occurences of significant rays near the ends of the spectrum. The resolution, while good, might be improved but this would need to come in the form of enhanced processing since practical considerations limit the size of the array.

Several general observations may be made about the results of the microwave measurements:

1. Under atmospheric multipath conditions, three paths are most likely to occur.
2. The angle-of-arrival of the strongest ray is generally elevated relative to the normal single-path value.
3. The AOAs of of the 2nd and 3rd strongest rays are observed to occur both above and below the normal value with the former predominantly elevated and the latter somewhat more likely to arrive at depressed angles.
4. The distribution of the separation in AOA of the two strongest rays is of some importance in diversity considerations. The evidence here suggests a most probable value for this separation in the range 0.15^{o} to 0.20^{o} (see Fig. II-14) with the stronger of the two about equally likely to be the higher or the lower (Fig. II-15).

The suggestion has been made [9] that ground reflections play a major role in the production of deep fading by interacting with a reduced amplitude (defocussed) direct ray - in effect, two path fading. There is some evidence in the present results to support this in that depressed angles are most readily accounted for by such reflections. Set against this is the fact that much of the output from the data analysis performed so far indicates a preponderance of multiple paths with suggested atmospheric origin. The automatic routines used though are not optimized to look for periods when reflections may be the predominant mechanism and this may prove to be a fruitful area to explore.

The need is there to gather more information on the occurrence and height distribution of layers such as is provided by the acoustic sounder. The indications are the such elevated layers are persistent in time (several hours), show periodic height variation (periods of several minutes upwards) and occur often as multiple layers. All of these properties have direct consequences for the propagation process and the simultaneous measurements outlined here will undoubtedly shed more light on the subject as further analysis progresses.

ACKNOWLEDGEMENTS.

The help provided by Ontario Hydro in allowing the use of the Uniondale tower is gratefully acknowledged as is similar aid afforded by Bell Canada with the Russelldale - London link.

REFERENCES

[1] W.T. Barnett, "Multipath Fading Effects on Digital Radio", IEEE Trans. Commun. Vol. COM-27, No. 12, pp. 1842-1848, December, 1979.

[2] A.B. Crawford and W.M. Sharpless, "Further Observations of the Angle-of-Arrival of Microwaves", Proc. IRE, Vol. 34, pp. 845-848, November, 1946.

[3] A.B. Crawford and W.C. Jakes, Jr., "Selective Fading of Microwaves", Bell System Tech. J., Vol. 31, No. 1, pp. 68-90, January, 1952.

[4] W.I. Lam and A.R. Webster, "Microwave Propagation on Two Line-of-Sight Oversee Paths", IEEE Trans. Antennas Propagation, Vol. AP-33, No. 5, pp. 510-516, May, 1985.

[5] H.G. Giloi, "A Study of Field Strength Height Profiles Caused by Multipath Fading", IEEE Trans. Antennas Propagation, Vol. AP-33, No. 12, pp. 1378-1385, December, 1985.

[6] A.R. Webster and A.M. Scott, "Angles-of-Arrival and Troposheric Multipath Microwave Propagation, "IEEE Trans. Antennas Propagation, Vol. AP-35, No. 1, pp. 94-99, January, 1987.

[7] Environment Canada Atmospheric Environment Services, Monthly Meteorological Summaries, London Airport, July-October, 1986.

[8] A.R. Webster, "Raypath Parameters in Tropospheric Multipath Propagation", IEEE Trans. Antennnas Propagation, Vol. AP-30, No. 4, pp. 796-800, July, 1982.

[9] R. L. Olsen, L. Martin, and T. Tjelta, "A Review of the Role of Surface Reflections in Multipath Propagation over Terrestrial Microwave Links.', Proc. NATO/AGARD Symposium on "Characteristics of Modern Sytems of Communications, Surveillance, Guidance and Control", Ottawa, 1986.

Transmitter:

Location	Uniondale, Ontario
Frequency	16.650 GHz
Power	80 mW
Antenna	0.6 m Diameter Parabolic Dish
Gain	37 dB
Beamwidth	2.0 Degrees
Height	45.7 m Above Ground 396 m Above M.S.L.
Polarization	Horizontal

Receiver:

Location	London, Ontario
Path Length	30.7 km

Reference Channel:

Antenna	0.6 m Diameter Parabolic Dish
Gain	37 dB
Beamwidth	2.0 Degrees
Height	24.5 m Above Ground 299 m Above M.S.L.
Polarization	Horizontal
Receiver Bandwidth	30 kHz
Dynamic Range	55 dB

Array Elements:

Antenna	Optimum Pyramidal Horns
Gain	20 dB
Beamwidth	Approximately 17 Degrees
Polarization	Horizontal
Number of Antennas	16
Antenna Separation	0.75 m
Receiver Bandwidth	13 kHz
Dynamic Range	55 dB

Table 1
The System Details

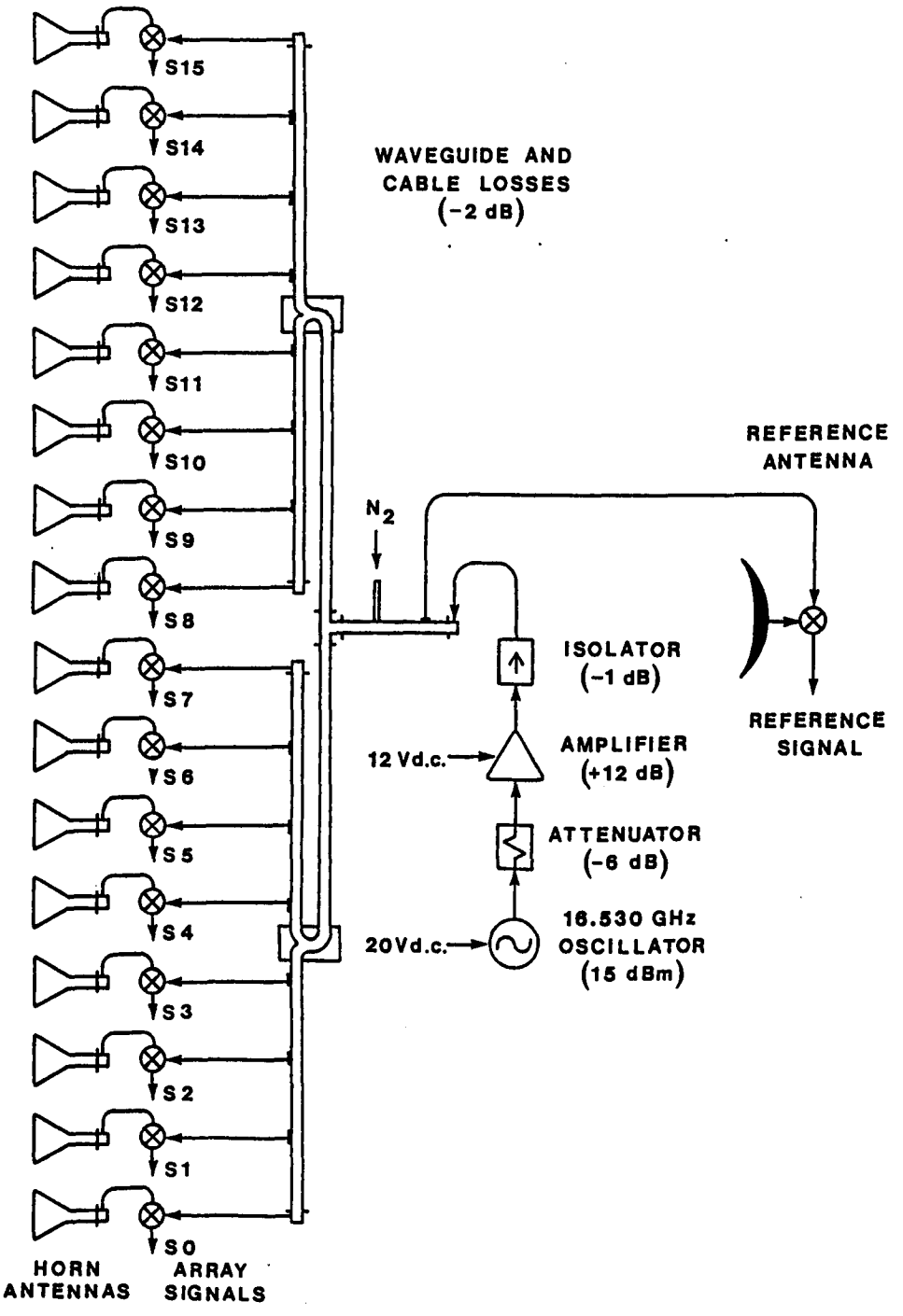

Fig. II-1 The local oscillator and waveguide arrangements.

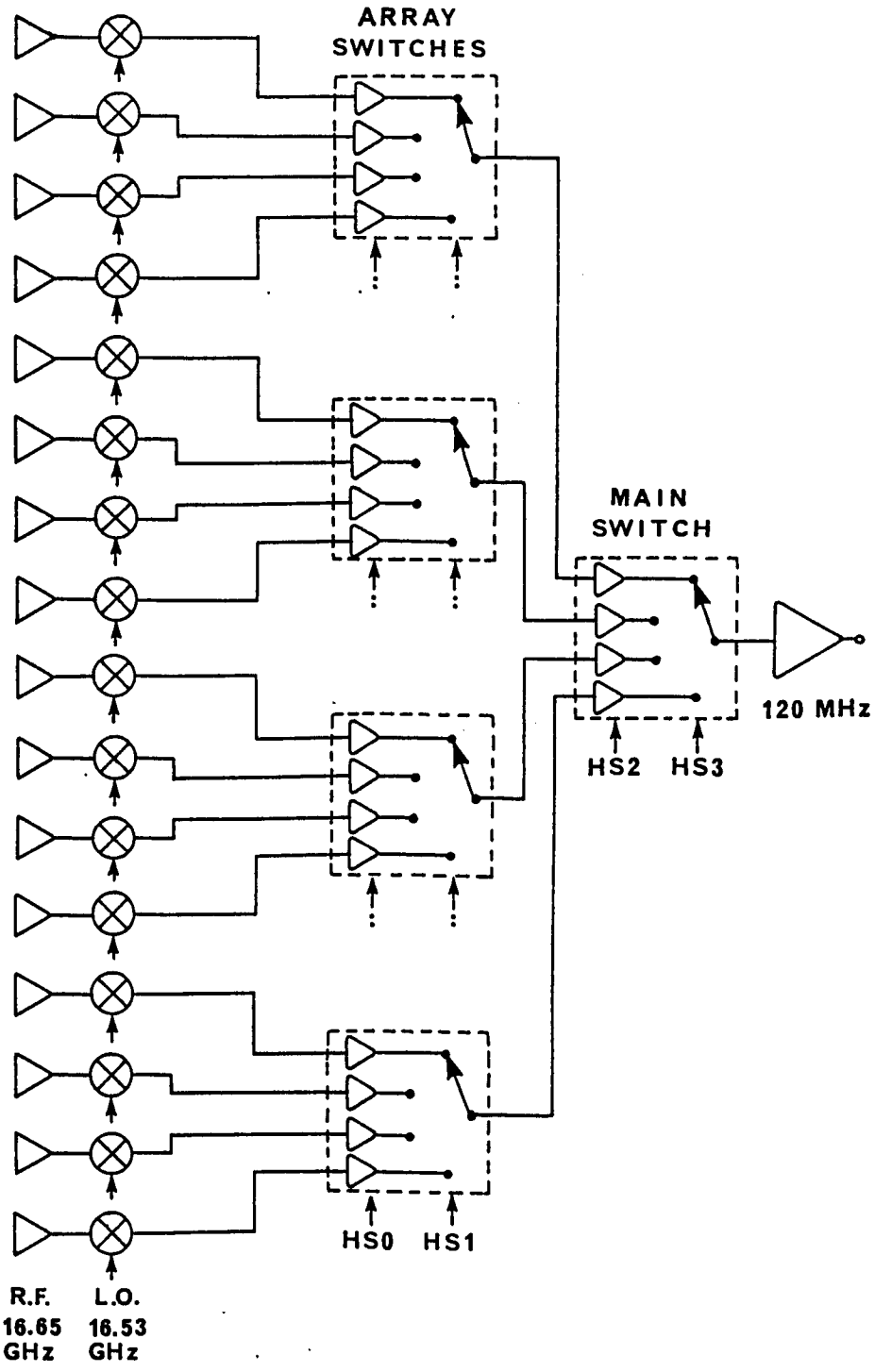

Fig. II-2 The array signal switching arrangements.

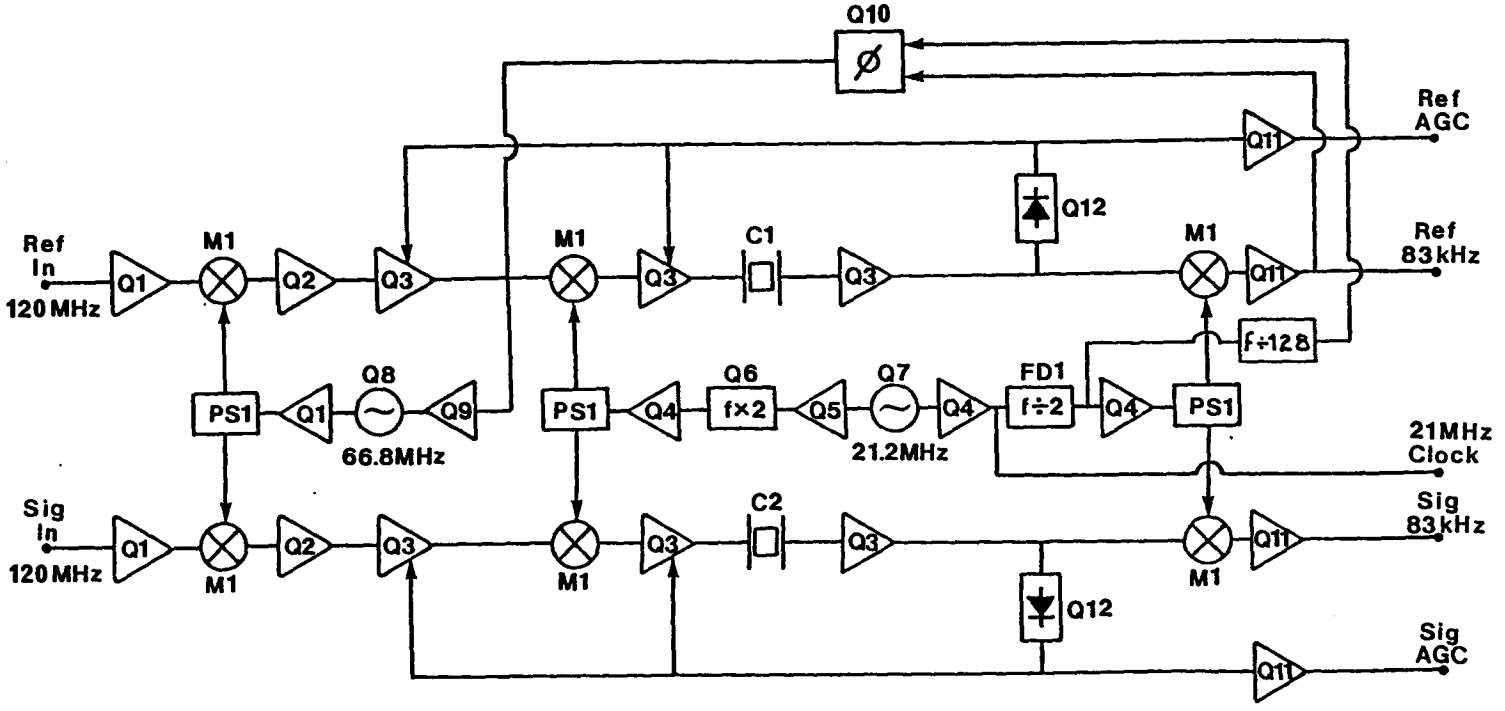

Fig. II-3 The receiver block diagram.

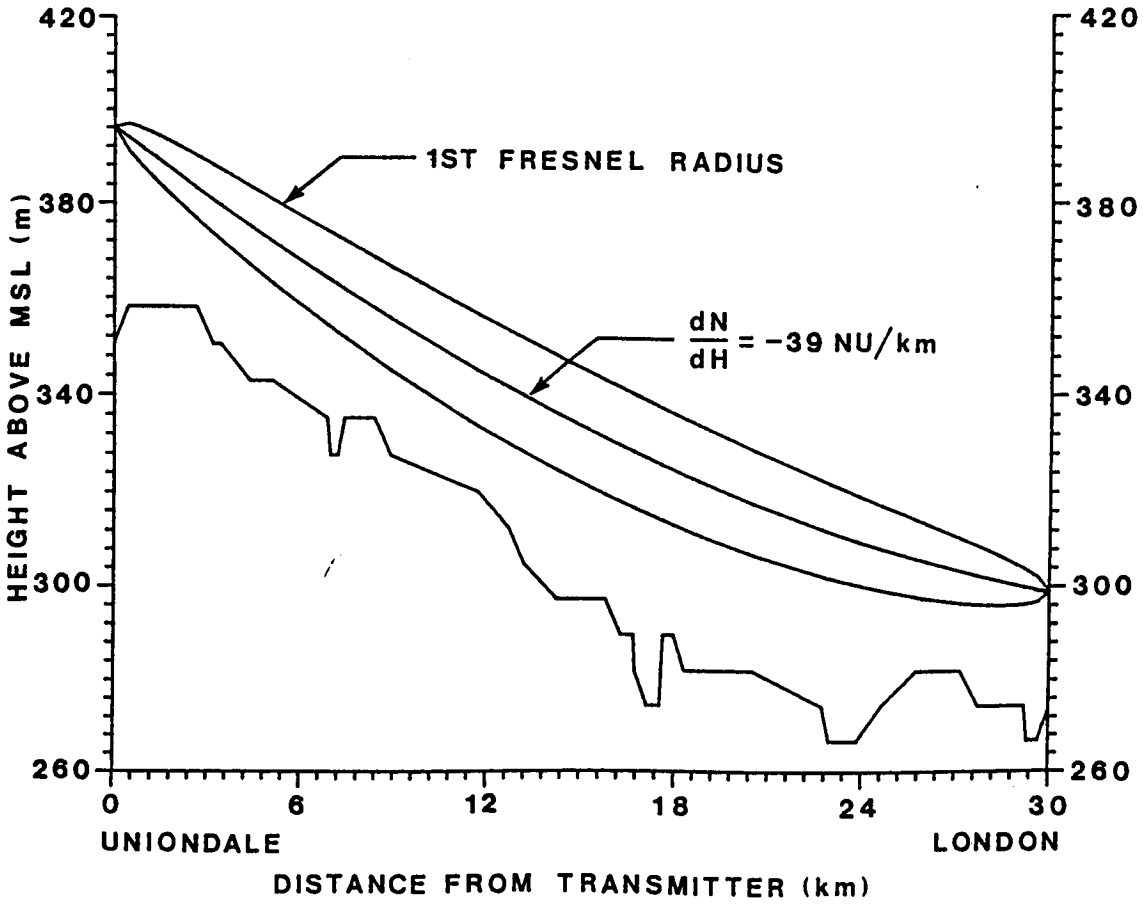

Fig. II-4 The path profile for the flattened earth, showing the propagation path and first Fresnel radius.

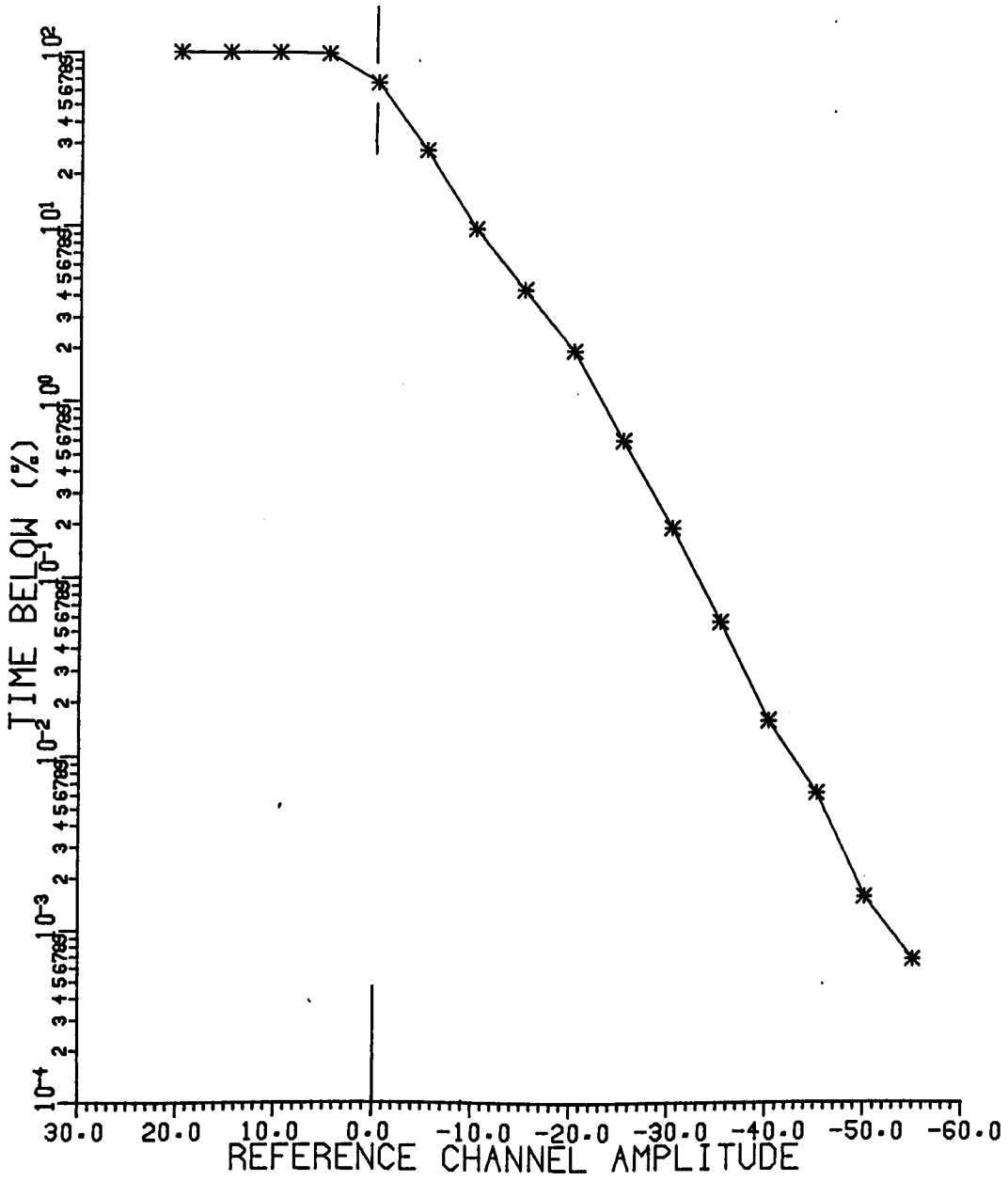

Fig. II-5 The cumulative distribution of the reference channel amplitude.

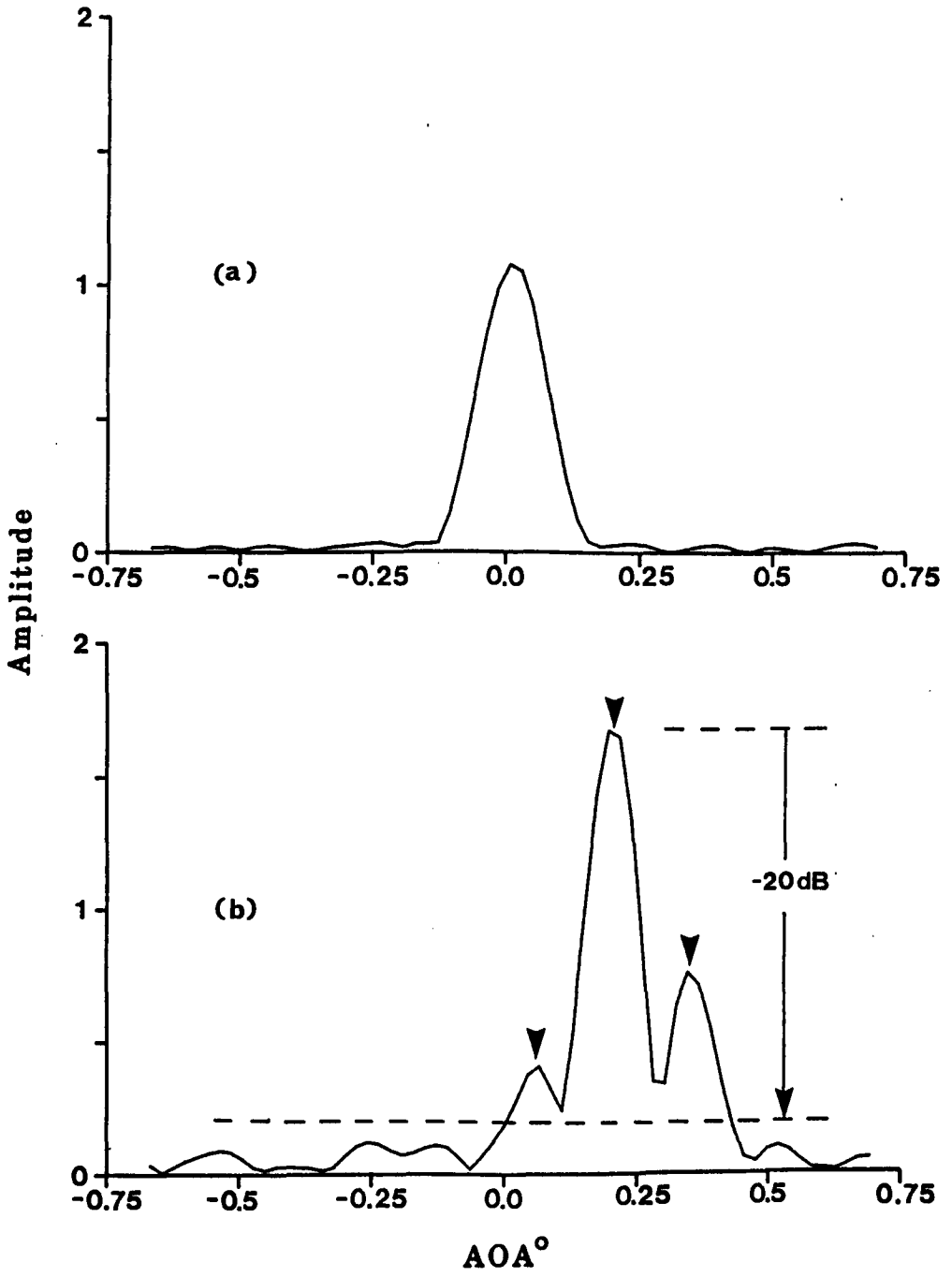

Fig. II-6 Angle-of-Arrival Spectra for a) normal propagation conditions, September 24, 1986, 00:20:00 EDT and b) multipath propagation conditions, September 2, 1986, 01:20:20 EDT.

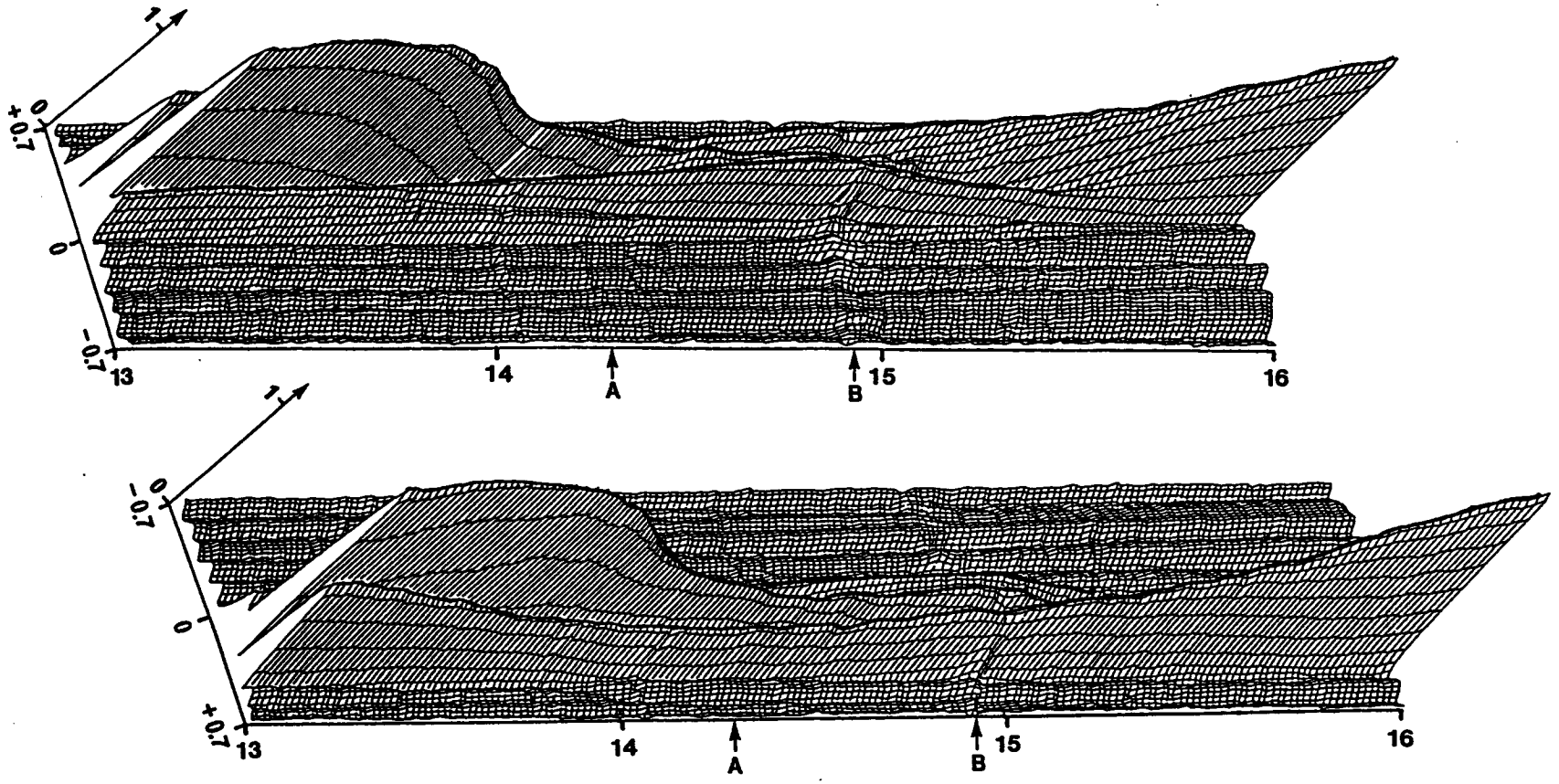

Fig. II-7 Angle-of-Arrival spectrum as a function of time for September 2, 1986, 01:13 to 01:16 EDT.

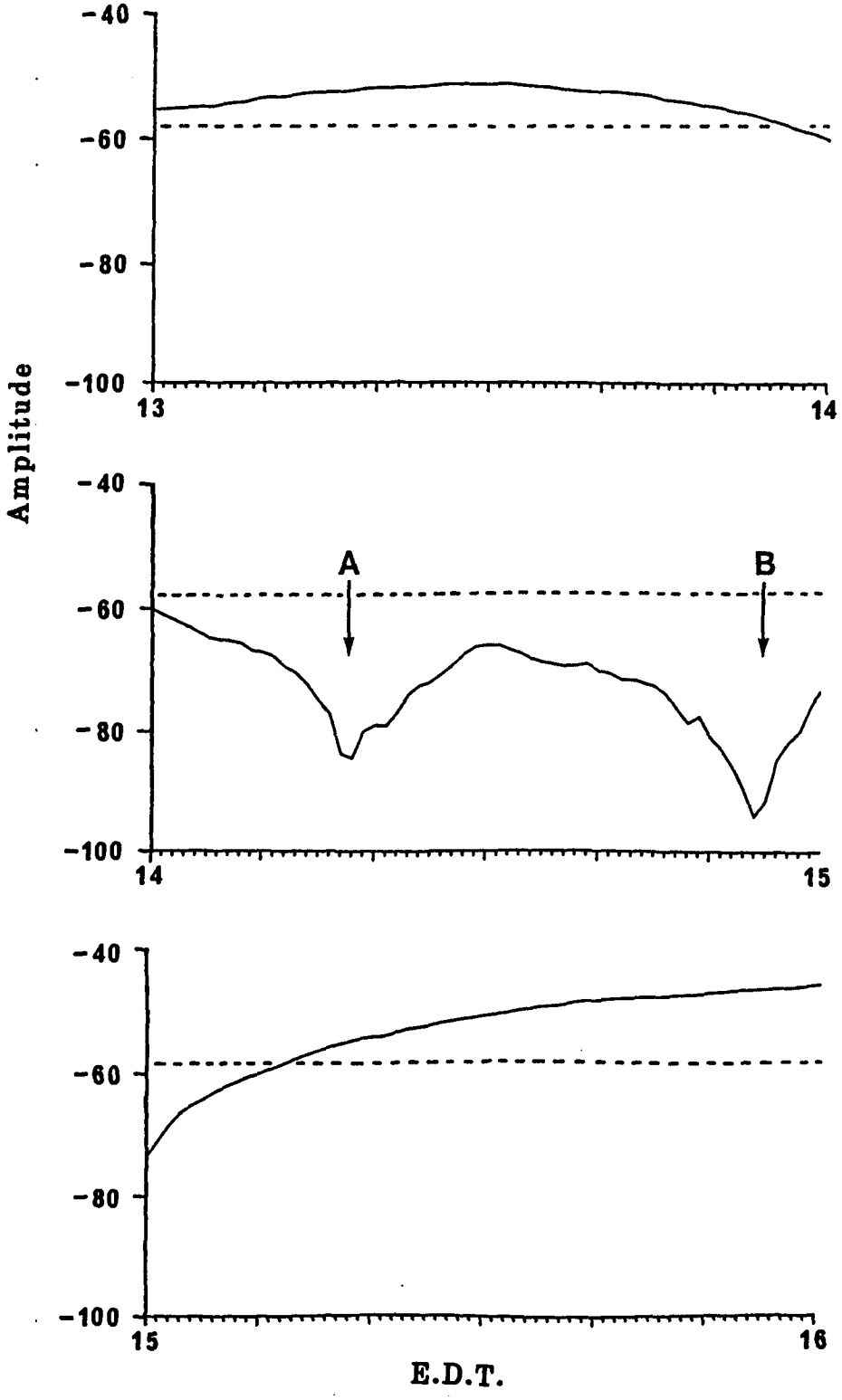

Fig. II-8 Reference channel amplitude for September 2, 1986, 01:13 to 01:16 EDT.

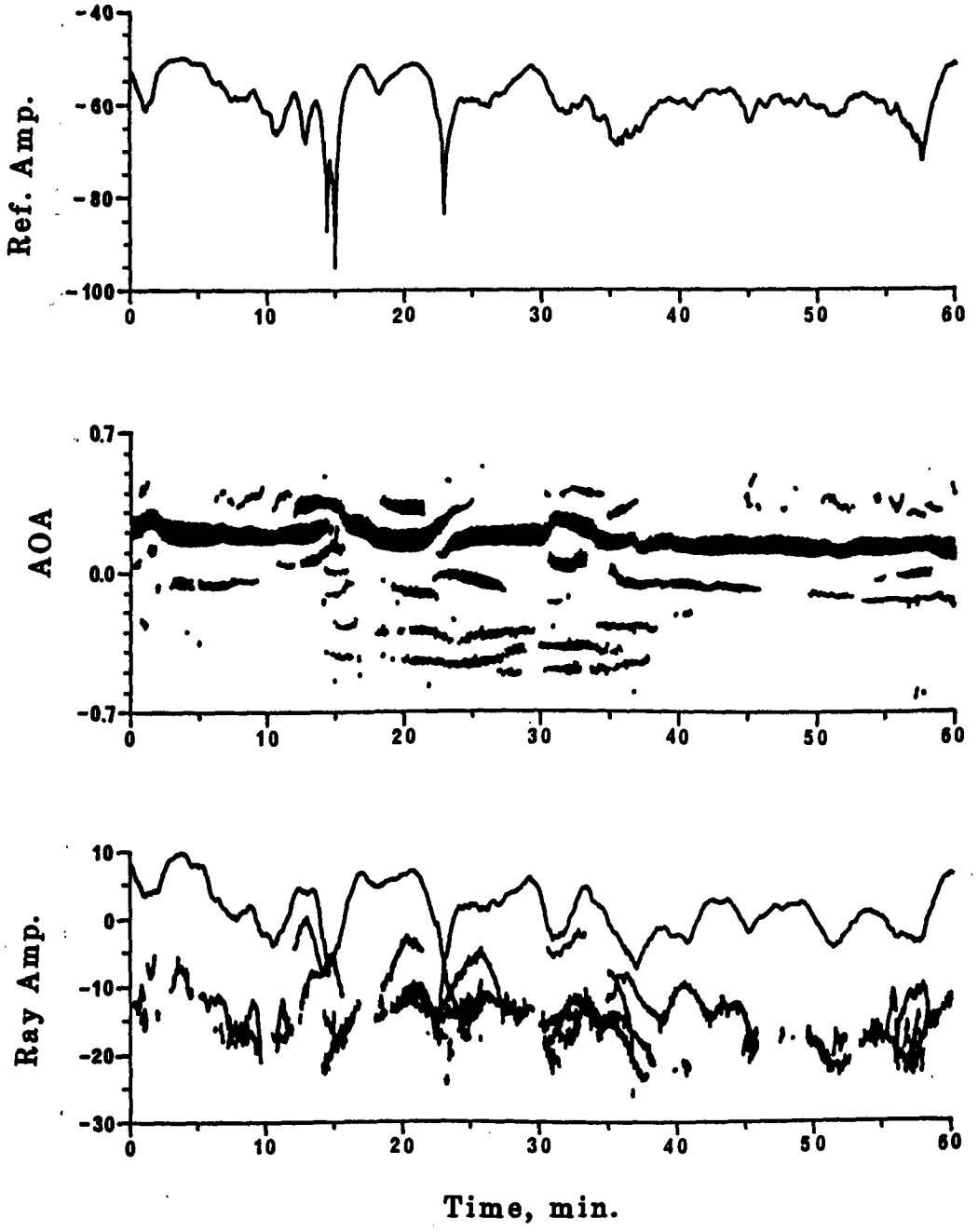

Fig. II-9 The a) reference channel amplitude b) angle-of-arrival, and c) ray amplitudes for September 2, 1986, 01:00 to 02:00 EDT.

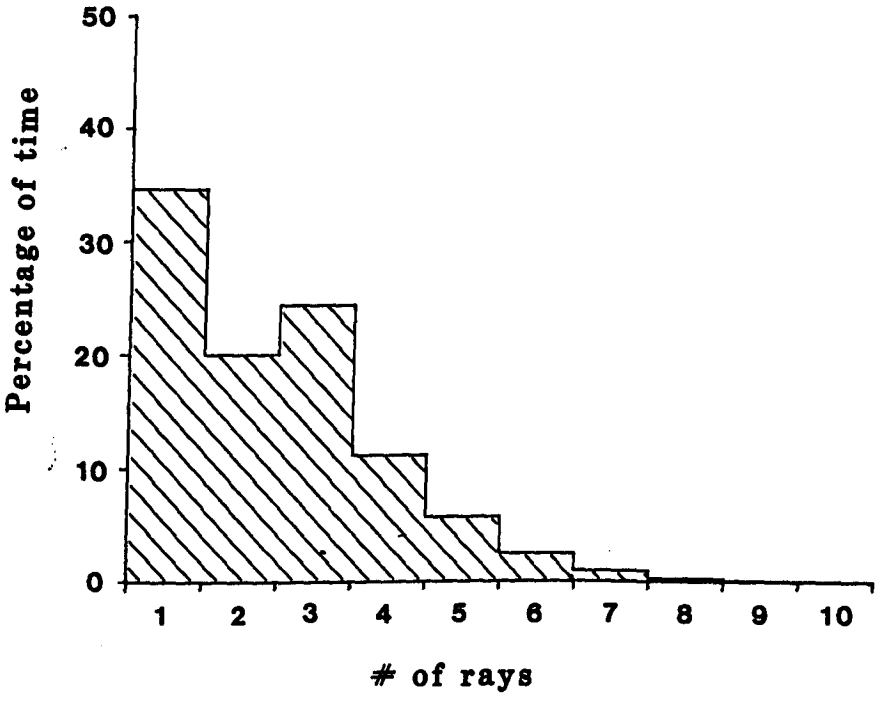

Fig. II-10 The distribution of the number of resolved propagation paths under multipath conditions.

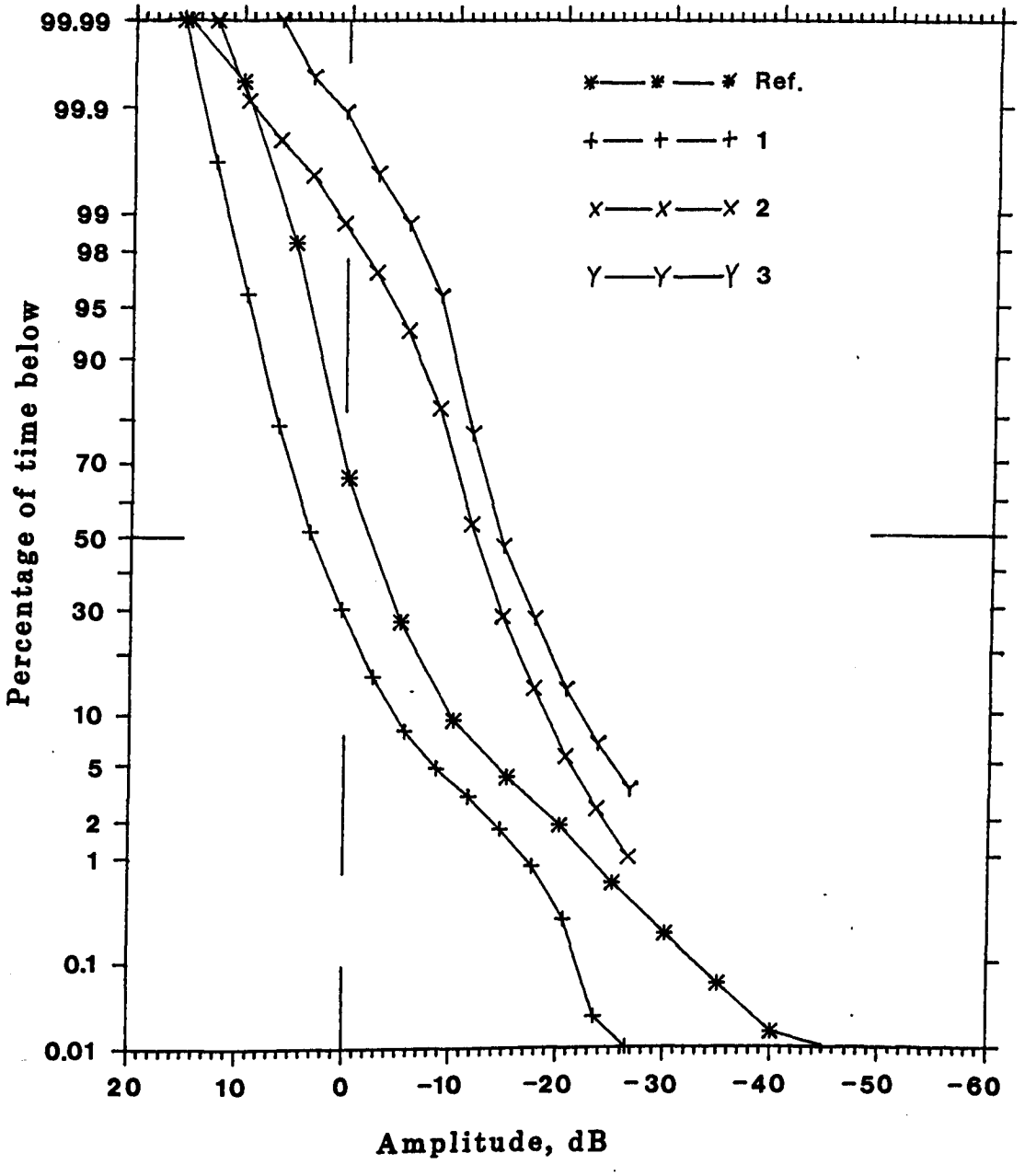

Fig. II-11 Cumulative distribution of the reference channel amplitude and the individual ray amplitudes; 1 is the strongest.

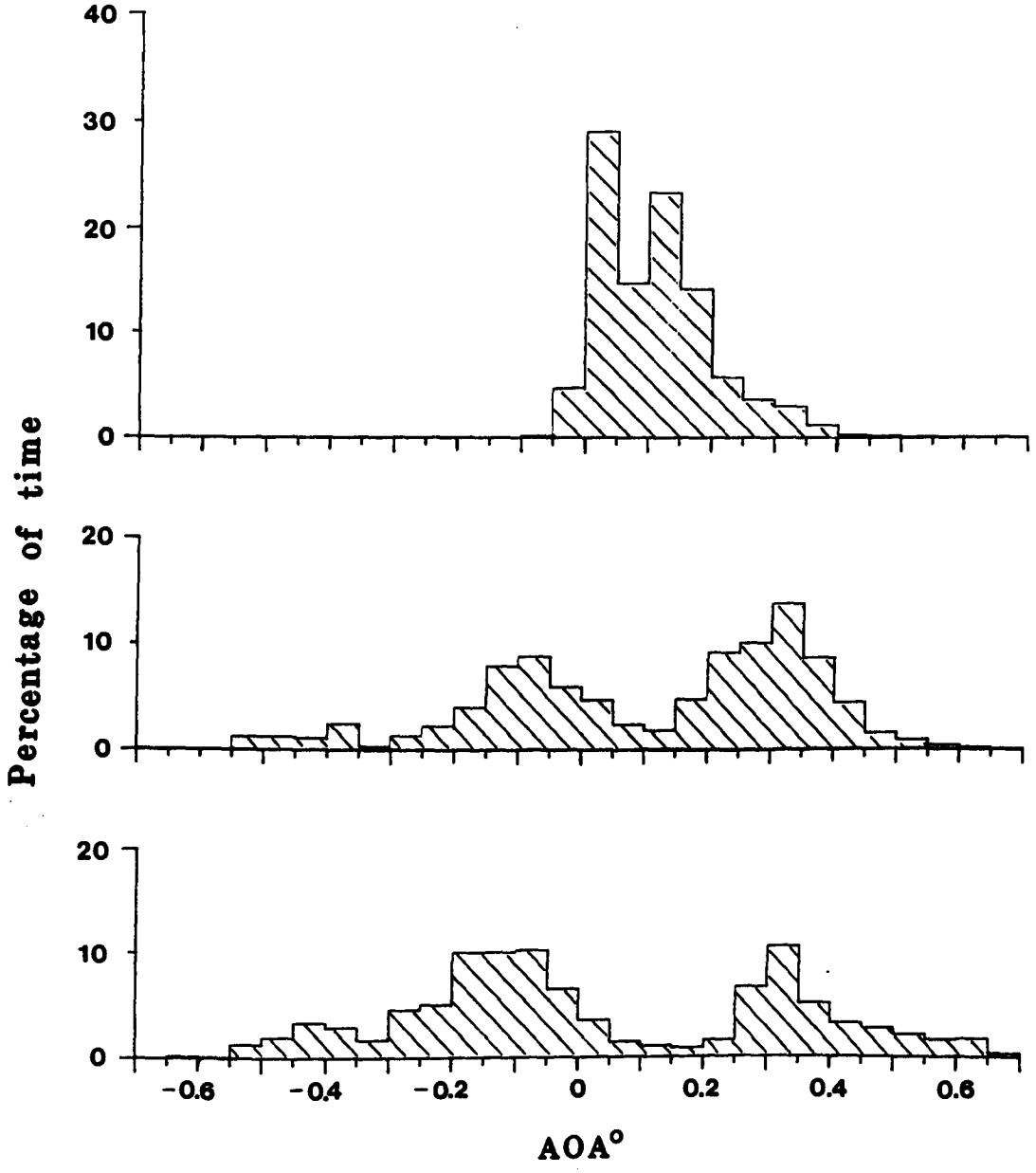

Fig. II-12 The distribution of angle-of-arrival for the a) strongest path, b) second strongest path, c) third strongest path.

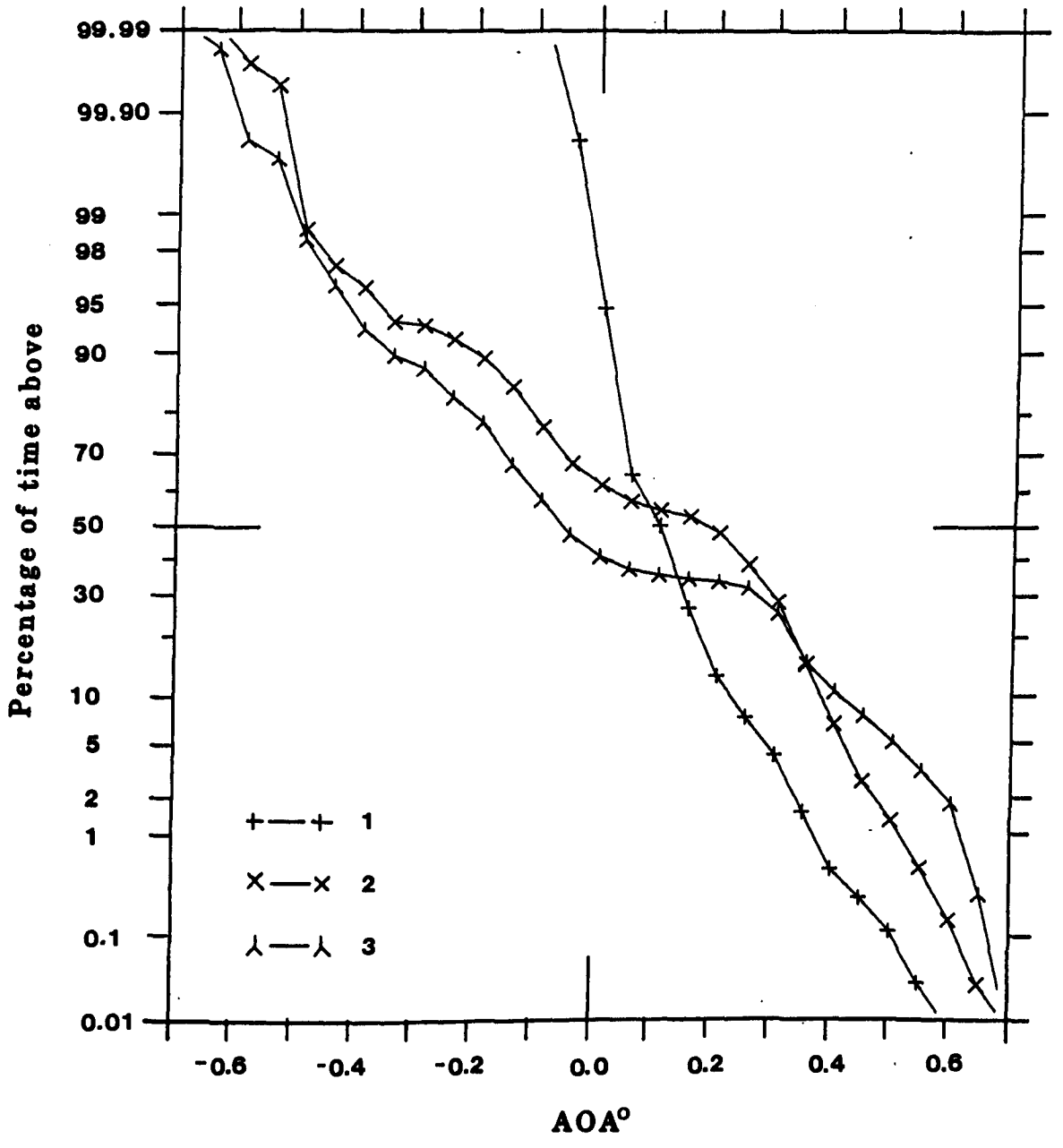

Fig. II-13 Cumulative distribution of the angle-of-arrival of the 1) strongest path, 2) second strongest path, 3) third strongest path.

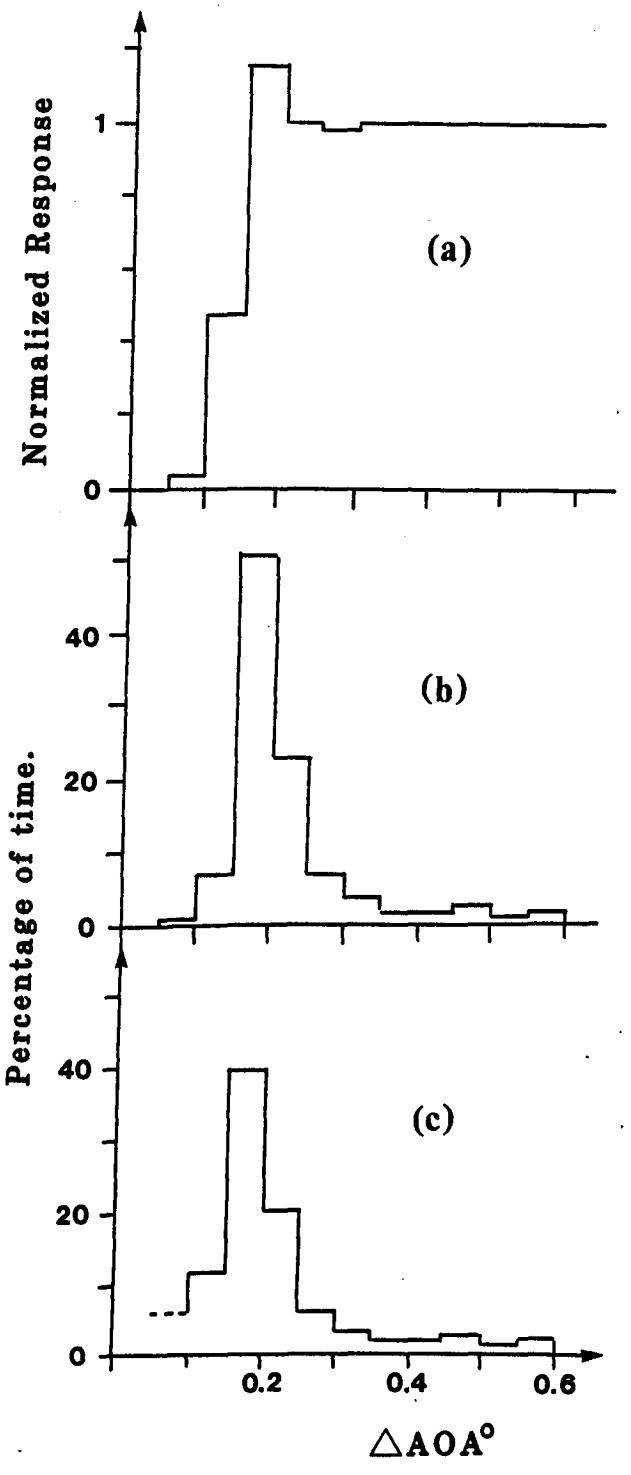

Fig. II-14 Separation in AOA between the two strongest rays in a multipath situation (0.05° intervals); a) the response of the processing technique to varied separation, b) the raw experimental results; c) experimental results corrected using (a).

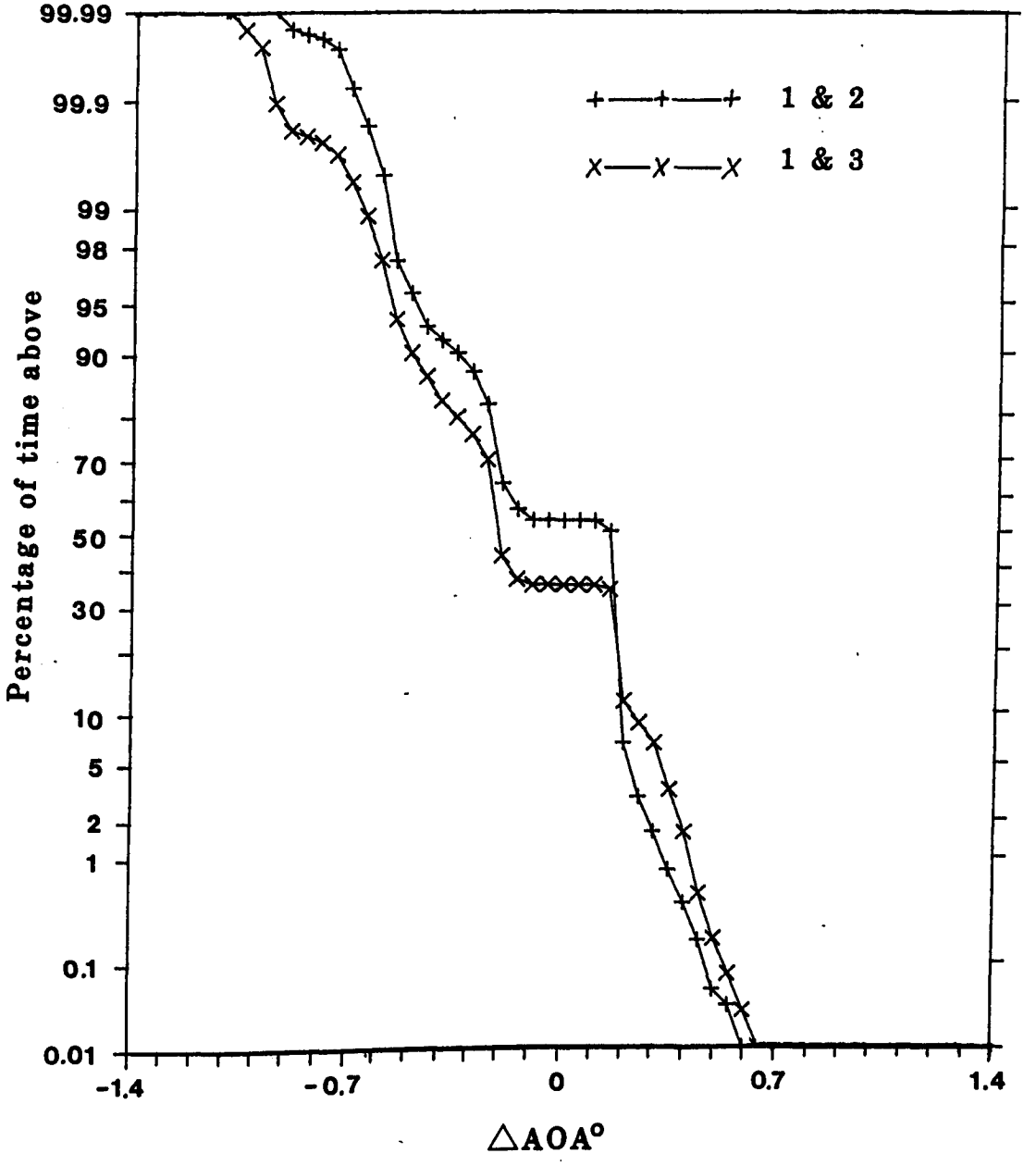

Fig. II-15 Cumulative distribution of the angle-of-arrival separation for the strongest and second strongest paths and the strongest and third strongest paths.

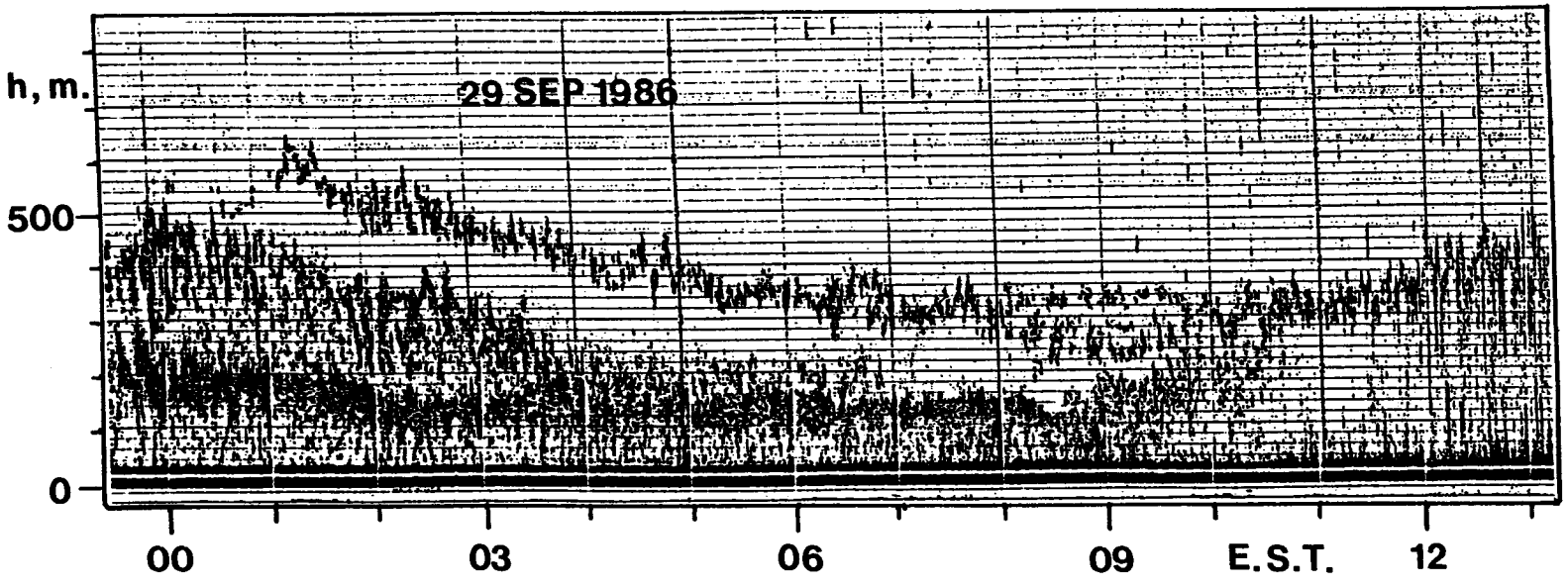

Fig. III-1 An original acoustic sounder record showing the occurrence of multiple layers.

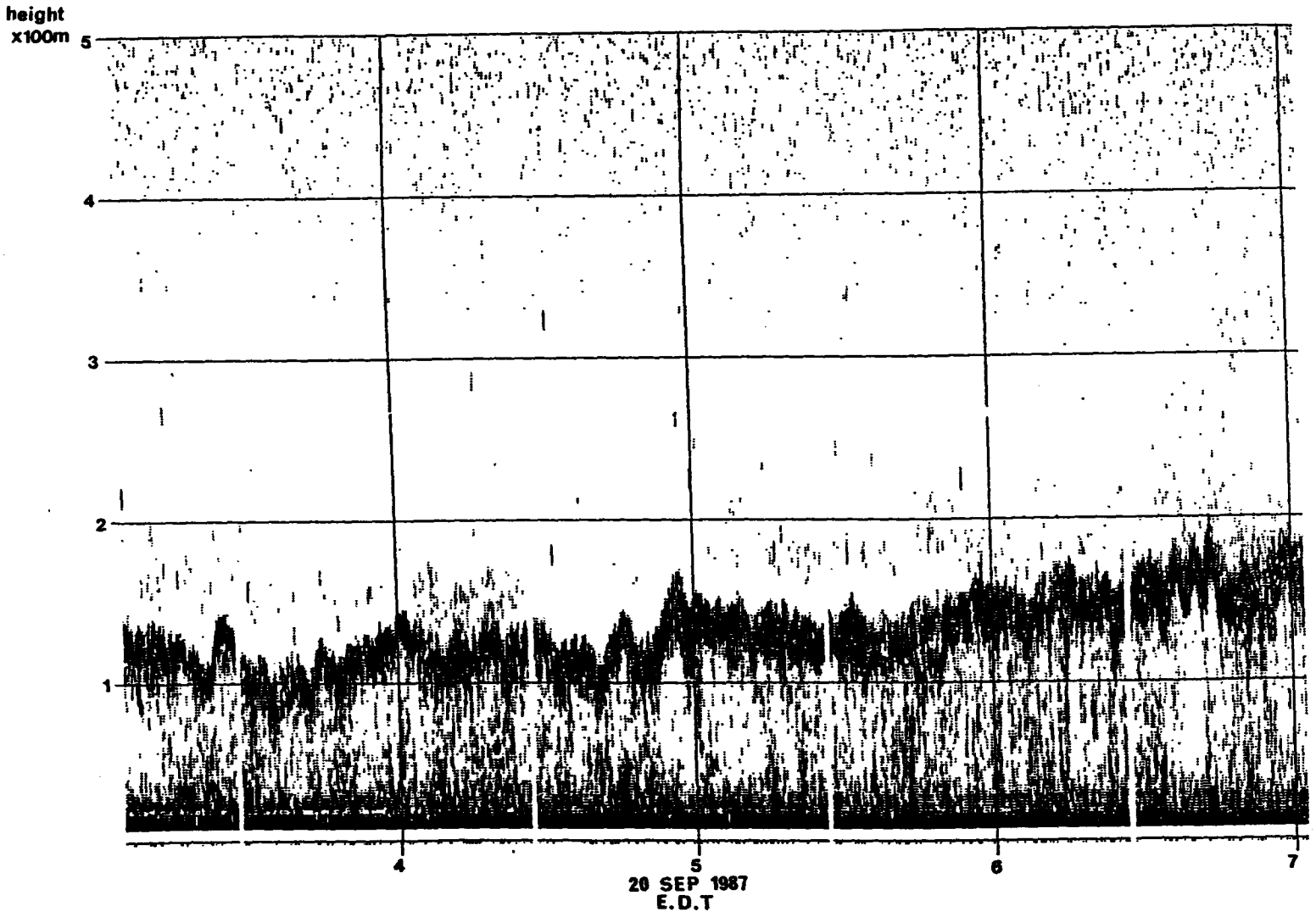

Fig. III-2 A digitized acoustic sounder record reproduced from a standard printer output.

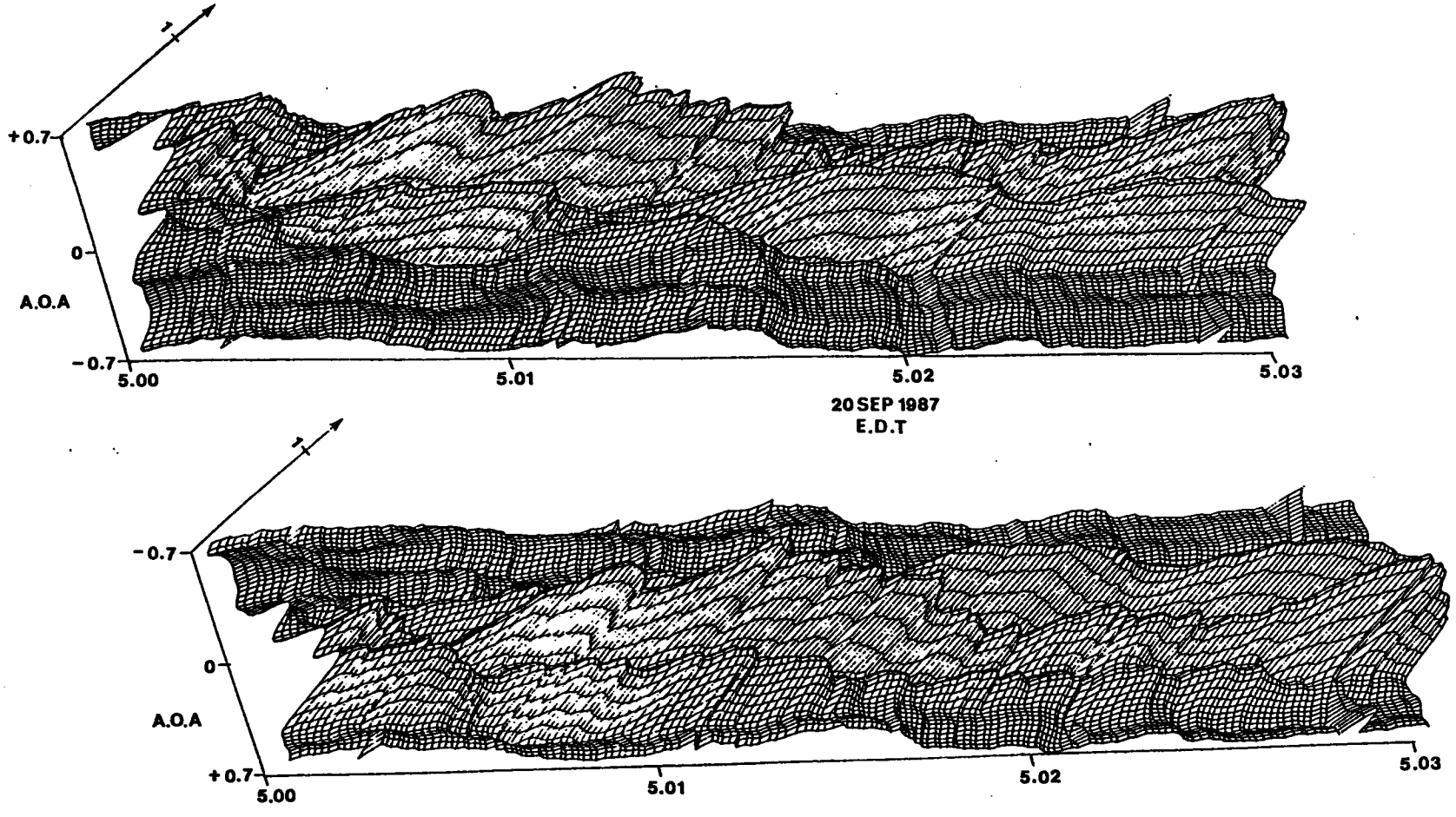

Fig. III-3 Angle of arrival record for a short period corresponding to the layer shown in Fig. III-2.